A NEW IMAGE DENOISING METHOD BASED ON THE BILATERAL FILTER

Ming Zhang and Bahadir Gunturk

Department of Electrical and Computer Engineering
Louisiana State University
Baton Rouge, LA 70803
Emails: mzhang4@lsu.edu, bahadir@ece.lsu.edu

ABSTRACT

In this paper we propose a new method to reduce noise in digital images. The method is based on the bilateral filter. The bilateral filter is a nonlinear filter that does spatial averaging without smoothing edges. The spatial averaging aspect of the bilateral filter is very crucial; the bilateral filter has been shown to work better than wavelet thresholding in some recent papers. The proposed method improves the bilateral filter through decomposing a signal into its frequency components. In this way, noise in different frequency components can be eliminated. Experimental results with both simulated and real images are given. In addition to this new method, we also provide an empirical study of the optimal parameter selection for the bilateral filter.

Index Terms— Image enhancement

1. INTRODUCTION

There are different sources of noise in a digital image. Among the noise sources, dark current noise is due to the thermally generated electrons at sensor sites. It is proportional to the exposure time and highly dependent on the sensor temperature. Shot noise is due the quantum uncertainty in photoelectron generation; and it is characterized by a Poisson distribution. Amplifier noise and quantization noise occur during the conversion of number of electrons to pixel intensities. The overall noise characteristics in an image depends on many factors, including sensor type, pixel dimensions, temperature, exposure time, and ISO speed. Noise is channel dependent. Typically, green channel is the least noisy and blue channel is the most noisy channel. (See Figure 1.) In single-chip digital camera, demosaicking algorithms are used to interpolate missing color components. That means, noise is in general not white. Noise in a digital image has low-frequency (coarse-grain) and high frequency (fine-grain) components. The high-frequency components are typically easier to remove; it is difficult to distinguish between real signal and low-frequency noise.

There have been many denoising methods developed over the years, such as the Wiener filter, wavelet thresholding [1], anisotropic filtering[2], bilateral filtering [3], total variation method [4], and non-local methods [5]. Among these methods, wavelet thresholding has been shown to be a highly successful method. In wavelet thresholding, a signal is decomposed into approximation (low-frequency) and detail (high-frequency) subbands, and the coefficients in the detail subbands are processed via hard or soft thresholding [1, 6, 7, 8]. The hard thresholding eliminates (sets to zero) coefficients that are smaller than a threshold; the soft thresholding shrinks the coefficients that are larger than the threshold as well. There are also other thresholding techniques in addition to hard and soft thresholding.

This work was supported in part by the National Science Foundation under Grant No 0528785.

Fig. 1. Portion of an image captured with a Sony DCR-TRV27; and its red, green, and blue channels. The blue channel is the most degraded channel. The noise apparently has low- and high-frequency components.

The main task of the wavelet thresholding is threshold selection. In the SURE Shrink approach [8], the optimal threshold value based on the Stein's Unbiased Estimator for Risk (SURE) is estimated. In the Bayes Shrink approach [9], the Bayesian Risk is minimized under the assumption of generalized Gaussian distribution for the wavelet coefficients. A major strength of the wavelet thresholding is the ability to treat different frequency components of an image separately; this is important because noise in real scenarios may be frequency dependent.

The bilateral filter was proposed in [3] and is an alternative to wavelet thresholding. It applies spatial weighted averaging without smoothing edges. This is achieved by combining two Gaussian filters; one filter works in spatial domain, the other filter works in intensity domain. Therefore, not only the spatial distance but also the intensity distance is important for the determination of weights. At a pixel location $\mathbf{x}$, the output of a bilateral filter can be formulated as follows:

$$\tilde{I}(\mathbf{x}) = \frac{1}{C} \sum_{\mathbf{y} \in \mathcal{N}(\mathbf{x})} e^{\frac{-\|\mathbf{y}-\mathbf{x}\|^2}{2\sigma_d^2}} e^{\frac{-|I(\mathbf{y})-I(\mathbf{x})|^2}{2\sigma_r^2}} I(\mathbf{y}), \qquad (1)$$

whereσ_d andσ_r are parameters controlling the fall-off of weights in spatial and intensity domains, $\mathcal{N}(\mathbf{x})$ is a spatial neighborhood of pixel $I(\mathbf{x})$, and C is the normalization constant:

$$C = \sum_{\mathbf{y} \in \mathcal{N}(\mathbf{x})} e^{\frac{-\|\mathbf{y}-\mathbf{x}\|^2}{2\sigma_d^2}} e^{\frac{-|I(\mathbf{y})-I(\mathbf{x})|^2}{2\sigma_r^2}}. \qquad (2)$$

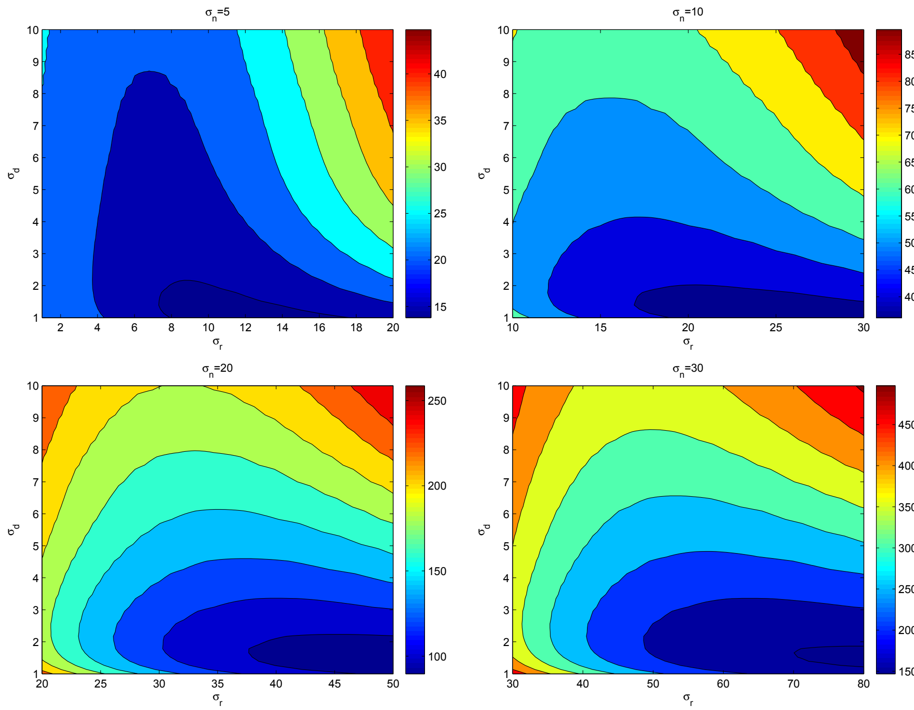

Fig. 2. The contour plots of the MSE values between the original image and the denoised image for different values σ_d, σ_r, and noise standard deviation σ_n. The test image is the standard gray-scale Lena image of size 512×512. From left to right, the noise standard deviations, σ_n, are 5, 10, 20, and 30. In each plot, the x axis is σ_r, the y axis is σ_d.

In addition to image denoising applications, bilateral filters have also been used in texture removal [10], tone mapping [11], volumetric denoising [12], and others. Elad [13] shows that the bilateral filter is a special case of the Jacob algorithm. This single iteration of Jacob algorithm, which is known as the diagonal normalized steepest descent, yields the bilateral filter. Durand and Dorsey [11] describes a liberalized version of the filter that speeds up the filter. They accelerate the bilateral filter by using a piecewise-linear approximation with FFT in the intensity domain and appropriate sub-sampling in the spatial domain. Paris and Durand [14] later derives an improved acceleration scheme for the filter. They express the filter in a higher-dimensioned space where the signal intensity is added to the original domain dimensions. The bilateral filter can be expressed as simple linear convolutions in this augmented space followed by two simple nonlinearities, so that they can derive simple criteria for down-sampling the key operations and achieve acceleration.

One weakness of the bilateral filter is not being able to remove salt-and-pepper type of noise. (Median filtering based operations have been proposed to eliminate this weakness.) A second drawback of the bilateral filter is its single resolution nature. Unlike the wavelet filter, the bilateral filter may not access to the different frequency components of a signal. Although it is effective in removing high-frequency noise, the bilateral filter fails to remove low-frequency noise. Another issue with the bilateral filter is that there is no theoretical work on the optimal values of the parameters, σ_d and σ_r.

This paper is organized as followed. In Section 2, we analyze parameters of the bilateral filter as a function of noise level. Based on some simulation results, we show that the value of σ_r is more important than the value of σ_d for varying noise levels. In Section 3 we will propose a multi-level bilateral filter based on wavelet decomposition. In Section 4, we compare the proposed method with Bayes Shrink [9], SURE Shrink [8] and the original bilateral filter [3]. The experiment results show that the multi-level bilateral filter works better than these methods visually.

2. PARAMETER SELECTION FOR THE BILATERAL FILTER

There are two parameters that control the behavior of the bilateral filter. Referring to (1), σ_d and σ_r characterizes the spatial and intensity domain behaviors, respectively. Although these parameters should be related to the noise and image characteristics, the issue has not been studied yet. In this paper, we made an empirical study of the optimal parameter values as a function of noise variance. We added white Gaussian noise to some standard images and applied the bilateral filter for different values of the parameters σ_d and σ_r. We repeated the experiment for different noise variances and recorded the mean squared error (MSE). A typical mean square error plot is given in Figure 2.

As seen in Figure 2, the optimal σ_d value is relatively insensitive to compared to the optimal σ_r. While σ_d value can be chosen as constant somewhere around 2; σ_r should be chosen as a function of σ_n. To see the relationship between σ_n and the optimal σ_r, we set σ_d to a constant, and plot the optimal σ_r values as a function of σ_n. Figure 3 shows plots for three standard images. As seen in these plots, σ_r and σ_n are linearly related to a great degree. σ_r is approximately equal to $1.7 \times \sigma_n$

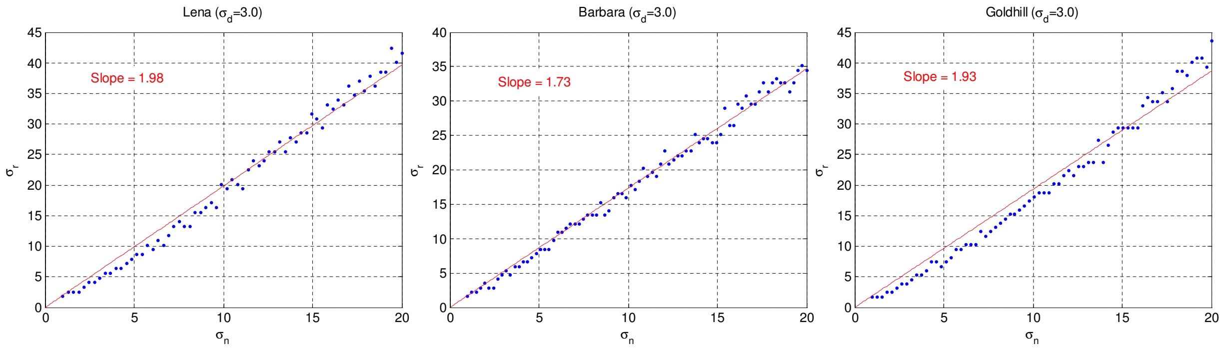

Fig. 3. The optimal σ_r values as function of noise standard deviation σ_n are plotted for three standard images. The image sizes are 512×512. The x axis is σ_n while the y axis is the σ_r that produces smallest MSE.

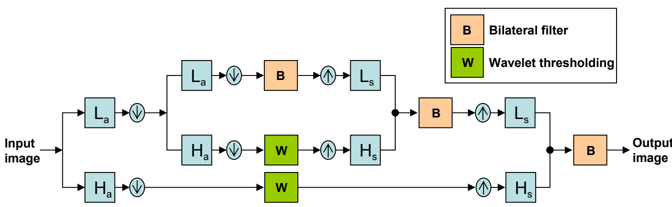

Fig. 4. Illustration of the proposed method. Image is decomposed into its low- and high-frequency components through analysis filters. Bilateral filter is applied to low-frequency components; wavelet thresholding is applied to high-frequency components.

3. PROPOSED METHOD

The denoising framework is illustrated in Fig 4. An image is decomposed into its frequency subbands with wavelet decomposition. (Note that the illustration treats the input as a one-dimensional signal and shows one approximation subband and one detail subband at each scale of the decomposition; in reality, there will be four subbands for a two-dimensional image at each scale.) The analysis and synthesis filters (L_a, H_a, L_s, and H_s) form a perfect reconstruction filter bank. The approximation subbands can be decomposed further; in the illustration, there are two levels of decomposition.

In the illustration, two types of filtering are applied on the image. The first one is the bilateral filtering, which is applied to the image and its approximation subbands. The second is the wavelet thresholding, which is applied to the detail subbands of the image. The multi-resolution bilateral filtering is a generalization of the standard bilateral filtering. It provides the capability to treat different frequency components of a signal individually. It is not necessary to use the same or correlated bilateral filter parameters at different scales. Bilateral filtering works in approximation subbands; however, some noise components can be identified and removed better in detail subbands, for example, salt-and-pepper type of noise. The wavelet thresholding part is optional but it provides this additional capability to the framework.

In the previous section, we have shown that the bilateral filter parameters should be related to the noise variance. There are different ways of estimating the noise levels in images and in different subbands of an image. In our experiments, we used the robust median estimator [1, 9] to estimate noise variance. The method fits the proposed framework well as it is also wavelet based. For the wavelet thresholding, we used the Bayes Shrink soft-thresholding method [9], which utilizes the same robust median estimator to determine threshold values.

4. EXPERIMENTAL RESULTS

These images were denoised using four methods. The first method is the BayesShrink wavelet thresholding algorithm [9]. Five decomposition levels were used; the noise variance is estimated using the robust median estimator [1]. The second method is the bilateral filter [3]. Based on our experiments discussed in the previous sections, we chose the following parameters for the bilateral filter: $\sigma_d = 1.8$, $\sigma_r = 2 \times \sigma_n$, and the window size is 11×11. The third method is the sequential application of [9] and [3]. The reason this method was included is to see the combined effect of [9] and [3] and compare it with the proposed method. The fourth method is the proposed method. For the proposed method, *db8* filters in Matlab were used for one-level decomposition. For the bilateral filtering part of the proposed method, we set the parameters as follows: $\sigma_d = 1.8$, the window size is 11×11, and $\sigma_r = 1.0 \times \sigma_n$ at each level. (In case of the original bilateral filter, $\sigma_r = 2 \times \sigma_n$ was a better choice. However, for the proposed method this lead to a smaller PSNR value on average. The reason is the double application of the bilateral filter in the proposed method. When σ_r was large, texture in the images was smoothed to produce low PSNR values. After some experimentation, $\sigma_r = 1.0 \times \sigma_n$ turned out to be better in terms of PSNR values. Here, we should note the fact that a higher PSNR does not necessarily correspond to a better visual quality.) For the wavelet thresholding part of the proposed method, the BayesShrink method [9] was used; and the noise variance was estimated again with the robust median estimator technique. To eliminate the border effects, images were mirror-extended before the application of the bilateral filter and cropped to the original size at the end. The PSNR results are given in Table 1.

In the second experiment, we captured a still image with a digital camera (Sony DCR-TRV27) in a low-light environment. We applied the denoising algorithms to this image. Figure 5 shows crop of this image and the denoising results for the Bayes Shrink, bilateral filter, and the proposed algorithm. As demonstrated in these experiments, the proposed method is producing very good visual results with real images.

Input Image	σ_n	BayesShrink [9]	Bilateral Filter [3]	[9] Followed by [3]	Proposed Method
Barbara 512×512	10	31.25	31.37	30.92	31.79
	20	27.32	27.02	27.16	27.74
	30	25.34	24.69	25.23	25.61
Boats 512×512	10	31.98	32.02	31.81	32.58
	20	28.55	28.40	28.43	29.25
	30	26.71	26.57	26.66	27.24
Goldhill 512×512	10	31.94	32.08	31.93	32.48
	20	28.69	28.90	28.80	29.50
	30	27.13	27.50	27.34	27.77

Table 1. PSNR comparison of the BayesShrink method [9], the bilateral filter [3], sequential application of the BayesShrink [9] and the bilateral filter [3] methods, and the proposed method. (The numbers are obtained by averaging the results of six runs.)

(a) (b) (c) (d)

Fig. 5. (a) Input image, (b) Original bilateral filter [3], (c) Bayes Shrink [9], (d) Proposed method with three-level decomposition.

5. CONCLUSIONS

In this paper we present a new image denoising method, which integrates the bilateral filter and the wavelet thresholding together. We decompose an image into low- and high-frequency components, and apply bilateral filtering on the approximation subbands and wavelet thresholding on the detail subbands. We have found that the optimal σ_r value of the bilateral filter is linearly related to the standard deviation of the noise. The optimal value of the σ_d is relatively independent of the noise power. Based on these results, we estimate the noise variance at each level of the subband decomposition and use the optimal σ_r value for bilateral filtering. The key factor in the performance of the proposed method is the multiresolution application of the bilateral filter. It helped eliminating the coarse-grain noise in images. The wavelet thresholding adds power the proposed method. We used a specific wavelet thresholding technique (i.e., the BayesShrink method); it is possible to improve the results further by using better detail-subband-denoising techniques or using redundant wavelet decomposition.

6. REFERENCES

[1] D. L. Donoho and I. M. Johnstone, “Ideal spatial adaptation by wavelet shrinkage,” *Biometrika*, vol. 81, no. 3, pp. 425–455, 1994.

[2] P. Perona and J. Malik, “Scale-space and edge detection using anistropic diffusion,” *IEEE Trans. Pattern Analysis and Machine Intelligence*, vol. 12, no. 7, pp. 629–639, July 1990.

[3] C. Tomasi and R. Manduchi, “Bilateral filtering for gray and color images,” in *Proc. Int. Conf. Computer Vision*, 1998, pp. 839–846.

[4] L. I. Rudin, S. Osher, and E. Fatemi, “Nonlinear total variation based noise removal algorithms,” *Physica D*, vol. 60, no. 1-4, pp. 259–268, 1992.

[5] A. Buades, B. Coll, and J. Morel, “Neighborhood filters and pde’s,” *Technical Report 2005-04, CMLA*, http://www.cmla.ens-cachan.fr/documentation/prepublications/2005.html, 2005.

[6] D. L. Donoho, “De-noising by soft thresholding,” *IEEE Trans. Information Theory*, vol. 41, pp. 613–627, May 1995.

[7] D. L. Donoho and I. M. Johnstone, “Adapting to unknown smoothness via wavelet shrinkage,” *Journal of the American Statistical Association*, vol. 90, no. 432, pp. 1200–1224, December 1995.

[8] D. L. Donoho, I. M. Johnstone, G. Kerkyacharian, and D. Picard, “Wavelet shrinkage: Asymptopia?,” *Journal of Royal Statistics Society, Series B*, vol. 57, no. 2, pp. 301–369, 1995.

[9] S. G. Chang, B. Yu, and M. Vetterli, “Adaptive wavelet thresholding for image denoising and compression,” *Trans. Image Processing*, vol. 9, no. 9, pp. 1532–1546, September 2000.

[10] B. M. Oh, M. Chen, J. Dorsey, and F. Durand, “Image-based modeling and photo editing,” in *Proc. SIGGRAPH*, 2001, pp. 433–442.

[11] F. Durand and J. Dorsey, “Fast bilateral filtering for the display of high-dynamic-range images,” in *Proc. SIGGRAPH*, 2002, pp. 257–266.

[12] W. C. K. Wong, A. C. S. Chung, and S. C. H. Yu, “Trilateral filtering for biomedical images,” in *Proc. International Symposium on Biomedical Imaging, IEEE*, 2004, pp. 820–823.

[13] M. Elad, “On the origin of the bilateral filter and ways to improve it,” *IEEE Trans. Image Processing*, vol. 11, no. 10, pp. 1141–1151, October 2002.

[14] S. Paris and F. Durand, “A fast approximation of the bilateral filter using a signal processing approach,” in *Proc. European Conference on Computer Vision*, 2006, pp. 568–580.